J. Am. Soc. Mass Spectrom. (2018) 29:78–84
DOI: 10.1007/s13361-017-1828-3

RESEARCH ARTICLE

Design and Application of a High-Temperature Linear Ion Trap Reactor

Li-Xue Jiang,[1,2] Qing-Yu Liu,[1,2] Xiao-Na Li,[1] Sheng-Gui He[1,2]

[1]Beijing National Laboratory for Molecular Sciences, State Key Laboratory for Structural Chemistry of Unstable and Stable Species, CAS Research/Education Center for Excellence in Molecular Sciences, Institute of Chemistry, Chinese Academy of Sciences, Beijing, 100190, People's Republic of China
[2]University of Chinese Academy of Sciences, Beijing, 100049, People's Republic of China

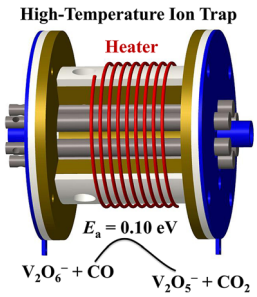

Abstract. A high-temperature linear ion trap reactor with hexapole design was homemade to study ion–molecule reactions at variable temperatures. The highest temperature for the trapped ions is up to 773 K, which is much higher than those in available reports. The reaction between $V_2O_6^-$ cluster anions and CO at different temperatures was investigated to evaluate the performance of this reactor. The apparent activation energy was determined to be 0.10 ± 0.02 eV, which is consistent with the barrier of 0.12 eV calculated by density functional theory. This indicates that the current experimental apparatus is prospective to study ion–molecule reactions at variable temperatures, and more kinetic details can be obtained to have a better understanding of chemical reactions that have overall barriers.

Keywords: Ion-molecule reactions, Mass spectrometry, Ion trap, CO oxidation, Variable temperature, Density functional theory

Received: 6 July 2017/Revised: 30 September 2017/Accepted: 2 October 2017/Published Online: 27 October 2017

Introduction

Gas-phase ion–molecule reactions performed under isolated, controlled, and reproducible conditions have been widely studied to uncover the mechanistic details of chemical processes in the related condensed phase [1–3]. Generally, chemical reactions that are overall barrierless can be studied at room temperature [4, 5]. However, the reactions that are thermodynamically favorable but kinetically slow or have overall barriers are difficult to be detected, and alternative technologies should be developed. For example, guided ion beam technology, a method to increase the collision energy, has been applied to measure not only the dynamic barriers of exothermic reactions but also the thermodynamics of endothermic reactions [6, 7]. Increasing the temperature of reaction systems is a prospective strategy to provide extra energies to overcome the barriers, and it is commonly used in the condensed phase, such as the Haber process and the catalytic transformation of methane [8, 9]. Thus, it is of great importance to explore high-temperature ion–molecule reactions in order to narrow the gaps between the gas-phase and related condensed-phase reactions.

It is technically challenging to control the temperature of gas-phase ions owing to the poor thermal conductivity of the vacuum system. Over the past decades, a variety of approaches have been explored to heat the ions [10–29]. The methods to heat the ions can be typically divided into two types. The first type is to heat the ions by passing through extension tubes of which the temperature can be variable [12–15]. In this way, the ions can be heated to a relatively higher temperature (~1200 K) because of the high efficiency of heat transfer of the high-pressure extension tubes. The second type is to use temperature-variable ion storage devices, such as ion drift tube [16–23], Fourier transform mass spectrometer [24], and ion trap [25–27]. For instance, Barran and co-workers developed a temperature variable ion mobility mass spectrometry to study the folding energetics of the trapped ions and the temperature of ions can be heated up to 520 K [18]. Ions trapped in a Fourier transform mass spectrometer can be heated to 488 K by elevating the temperature of the vacuum chamber [24]. Furthermore, various methods have been proposed to heat the ions

Electronic supplementary material The online version of this article (https://doi.org/10.1007/s13361-017-1828-3) contains supplementary material, which is available to authorized users.

Correspondence to: Xiao–Na Li; *e-mail:* lxn@iccas.ac.cn, Sheng–Gui He; *e-mail:* shengguihe@iccas.ac.cn

trapped in an ion trap [25–29]. McLuckey et al. used a temperature variable bath gas to heat the ions and the temperature of the trapped ions can be up to 493 K [25]. A heater has been inserted near the trapping electrodes by Glish et al. to heat both of the bath gas and the electrodes, and the trapped ions can be heated up to 443 K [26]. Gerlich et al. and Anderson et al. used lasers to heat the ions in the quadrupole ion trap [28, 29]. Recently, Gronert et al. developed a temperature variable ion trap mass spectrometer by applying polyimide-coated heating elements to the end-cap electrodes of a Bruker Esquire ion trap system, and the temperature of ions can be up to 373 K [27]. Note that the temperature of the trapped ions heated in the ion storage devices was much lower with respect to that heated by the extension tubes (520 K versus 1200 K) [12]. Thus, higher-temperature ion storage devices should be developed to study the reactivity of mass-selected ions in a larger range of temperatures.

Herein, a high-temperature linear ion trap (LIT) reactor was homemade by twining a resistive heater around the outside shell of the ion trap reactor to heat the hexapole rods and end-cap electrodes. With this design, the mass-selected ions in the reactor can be heated up to 773 K. The performance of the apparatus has been evaluated by studying the reaction of $V_2O_6^-$ cluster anions with CO at different temperatures. The apparent activation energy of 0.10 ± 0.02 eV was determined, which is consistent with the results of density functional theory (DFT) calculations.

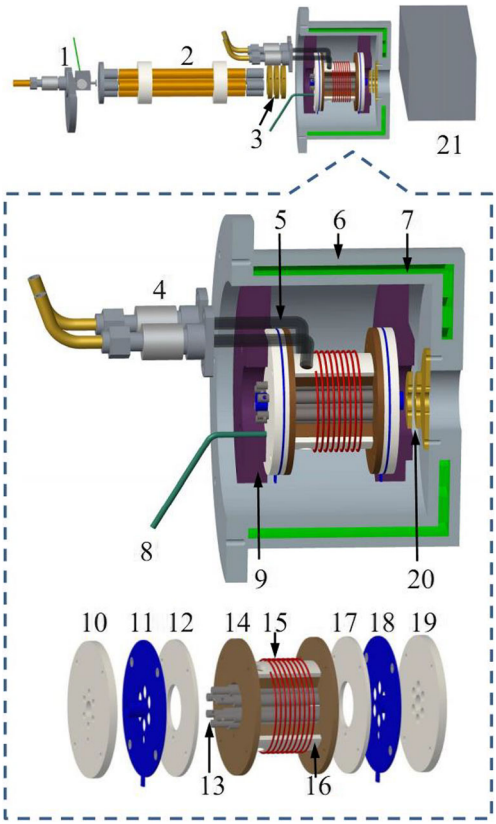

Figure 1. A schematic presentation of the high-temperature ion trap reactor. Parts: 1, cluster source; 2, quadrupole mass filter; 3 and 20, ion focusing assembly; 4, pulsed valves; 5, quartz glass tubes; 6, cooling water container; 7, cooling water; 8, thermocouple; 9, thermal insulator (SiO_2 ceramics); 10, 12, 16, 17, and 19, electronic insulator (Al_2O_3 ceramics); 11 and 18, cap electrodes; 13, hexapole rods; 14, cell for confining the bath gas and reactant gas; 15, resistive heater; 21, reflectron time-of-flight mass spectrometer

Experimental and Theoretical Methods

Experimental Details

A schematic presentation of the experimental apparatus is shown in Figure 1. The cluster source (Part 1), the quadrupole mass filter (Part 2), and the time-of-flight mass spectrometer (TOF-MS) (Part 21) are the same as those used in our previous works [30, 31], whereas the high-temperature LIT assembly (Parts 4–20) was newly designed in this work.

A brief introduction of the experiment is given below. The vanadium oxide clusters were generated by pulsed laser ablation of a rotating and translating vanadium disk in the presence of 1.0% O_2 seeded in a He carrier gas (99.999%) with a backing pressure of about 5.0 atm. The $V_2O_6^-$ anions were mass-selected by the quadrupole mass filter and entered into the LIT where they were confined, heated, and then interacted with a pulse of CO for about 3.0 ms. Longer heating time did not change the relative intensities of product ions, indicating that the ions have been thermalized. The temperature of the LIT reactor can be heated from 300 to 773 K. The ions ejected from the LIT reactor were detected by the reflectron TOF-MS.

The principles to run the linear multipole ion traps can be found in a previous study [32]. The LIT assembly contains a set of hexapole rods (Part 13) and two end-cap electrodes (Parts 11 and 18). The hexapole rods were insulated from each other by two pieces of Al_2O_3 ceramics (Parts 10 and 19) and they were put together into a gas cell (Part 14) that can confine the bath gas and reactant gas. Two quartz glass tubes (Part 5) were used to deliver the bath gas and reactant gas into the gas cell, and the pressure of gases were controlled by two pulsed valves (Part 4, General Valve, Series 9). Al_2O_3 ceramics functions as a good electric insulator and heat conductor. Thus, it is widely used in our high-temperature LIT, as shown in Figure 1. Two pieces of Al_2O_3 ceramics (Parts 12 and 17) were inserted between the two end-cap electrodes and hexapole rods, and the gas cell was hugged by two pieces of semi-circles of Al_2O_3 ceramics (Part 16). A resistive heater (Part 15, Nichrome 80/20) was crossed around the semi-circles of Al_2O_3 ceramics to heat the ion trap assembly. The electrodes and the gas cell are made of molybdenum that is stable at high temperatures. A K-type thermocouple (Part 8) that can function in the temperature range between 73 and 1623 K was inserted into the wall of the gas cell to monitor the temperature of the ion trap. A cooling water system (Parts 6 and 7) was designed to protect the vacuum chamber of the mass spectrometer. The entire ion trap assembly was fixed by two pieces of SiO_2 ceramics (Part 9), which is a good thermal insulator at high temperatures. The power of the resistive heater can be up to 100 W. The temperature of ion trap

can be varied by 4–6 K in 1 min. However, in this study, sufficient time was used to insure thermal equilibrium. The temperature of the LIT can be varied from 300 to 773 K using the resistive heater, which was controlled by a programmable proportional-integral-derivative (PID) controller (YURON, YL611).

In our experiments, both of the collision gas (He) and reactant gas (CO), were delivered with the pulsed rather than the continuous mode. This design can save the gases and keep a good vacuum for the TOF-MS. However, it becomes difficult to measure the instantaneous number density inside the trap reactor. The following equations can be used to estimate the number density (n) inside the ion trap [33]:

$$n = \frac{N_{\max}}{V} e^{-(t-t_c)/\tau} \quad (1)$$

$$N_{\max} = N_{total} \frac{\tau}{\delta t} \left(1 - e^{-\delta t/\tau}\right) \quad (2)$$

$$\tau = \frac{V}{2CS} \quad (3)$$

where $N_{\max}$ is the instantaneous molecular number in the trap at the time (t_c) that the pulsed valve is closed, which corresponds to a maximal molecular number caused by the gas pulse, τ is the decay time for the flowing of the gas from the trap to the vacuum, N_{total} is the number of molecules injected into the trap within the pulse width of δt, V (1.62×10^4 mm^3) is the volume of the trap, S (12.56 mm^2) is the cross-sectional area defined by the aperture through which the cluster ions enter into and come out of the trap, and the speed of sound C can be calculated under the approximation of ideal gas as $C = (\gamma kT/m)^{1/2}$, in which γ is the adiabatic index, k is the Boltzmann constant, T is the temperature, and m is the mass of the gas molecule.

The reaction time t_R is set to be smaller than or on the order of the decay time τ_R so that the molecular number does not change greatly during the reaction in the trap. Assuming pseudo-first-order reaction between the cluster and the reactant molecules, the rate constant (k_1) can be determined by the following equation of which the derivation is omitted for clarity [33]:

$$\ln\frac{I_R}{I_T} = -k_1 \frac{N_{\max}}{V} \tau_R \left[1 + \frac{\delta t_R}{2\tau_R} - e^{-(t_R - \delta t_R)/\tau_R}\right] \quad (4)$$

in which I_R is the intensity of the reactant cluster ions after the reaction and I_T is the total ion intensity including product ion contribution. It can be seen that the $\ln(I_R/I_T)$ value is proportional to molecular number $N_{\max}$ rather than reaction time t_R.

The uncertainties of $\ln(I_R/I_T)$, τ_R, V, and t_R are about 10%, 15%, 5%, 5%, respectively. The $N_{\max}$ can be systematically under- or overestimated by 40% in our experiments. As a result, the uncertainties of relative rate constants in this study are within 20%, whereas the uncertainties of the absolute values are within 50%. The pseudo-first-order rate constants (k_1) determined in this study can be compared with those in our previous reports. For example, the k_1 values determined herein for the reactions of $V_2O_6^-$ anions with C_2H_4 and C_3H_6 at room temperature are 3.7×10^{-13} and 3.8×10^{-12} cm^3 molecule^{-1} s^{-1}, respectively, which are comparable with the values of 5.3×10^{-13} and 5.9×10^{-12} cm^3 molecule^{-1} s^{-1} determined in our previous study [33]. The discrepancy between the rates that are reported in this study and the one used in our previous study can be attributed to two factors: (1) the experimental uncertainties, and (2) the different pressures of the collision gas (He). In recent studies [34], we found that the larger pressure of collision gas benefits the formation of adsorption product. For the reactions of $V_2O_6^-$ with C_2H_4 and C_3H_6, the major reaction channels are molecular adsorption. When $V_2O_6^-$ reacts with C_2H_4 and C_3H_6, the number density of collision gas (He) becomes much smaller than the previous study because of the shorter decay time. Thus, the rate constants can be smaller than the ones in the previous study.

Computational Details

The DFT calculations using the Gaussian 09 program [35] were carried out to study the mechanism for the reaction of $V_2O_6^-$ anions with CO. The B3LYP functional [36, 37] with TZVP basis sets [38] was used. The same functional and basis sets have been adopted successfully for many reaction systems involving vanadium oxide clusters [33, 39, 40]. The relaxed potential energy surface scans [41] were used to obtain the good guess structures for the intermediates (IMs) and the transition states (TSs) along the pathways. The TSs were optimized using the Berny algorithm method [42]. Vibrational frequency calculations were performed to check that each of the IMs or TSs has zero or only one imaginary frequency, respectively. Intrinsic reaction coordinate calculations were carried out so that each TS connects two appropriate local minima. The zero-point vibration corrected energies (ΔH_0) are reported in this work.

Results and Discussion

The TOF mass spectra for the interactions of laser ablation generated and mass-selected $V_2O_6^-$ cluster anions with CO at different temperatures are shown in Figure 2. The TOF mass spectra for the reaction of $V_2O_6^-$ cluster anions with CO at different reaction times are shown in Figures S1 and S2 (Supporting Information). On the interaction of $V_2O_6^-$ anions with Ar at 773 K, no product peak was generated (Figure 2a). This indicates that the $V_2O_6^-$ cluster is stable enough at the high temperature up to 773 K. Upon the interaction of $V_2O_6^-$ with CO at 298 K, a very weak peak that can be assigned as $V_2O_5^-$ can be observed, suggesting that $V_2O_6^-$ can oxidize one CO molecule to give rise to product $V_2O_5^-$ (Reaction 5). The relative ion intensity of $V_2O_5^-$ increased apparently with the increase of the reaction temperature. It should be noted that the ions will keep heated by the thermal radiation of the gas cell

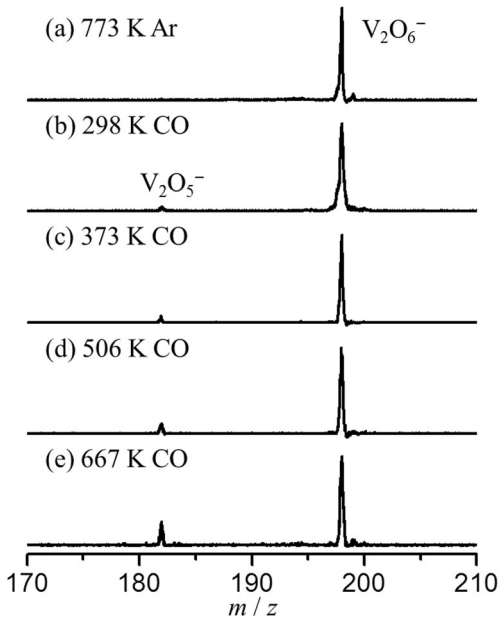

Figure 2. TOF mass spectra for the interactions of laser ablation generated and mass-selected $V_2O_6^-$ cluster anions with **(a)** Ar and **(b)-(e)** CO at different temperatures. The reaction time is about 2.0 ms **(b)** and 3.0 ms **(c)-(e)**. The maxmum molecule density of CO in the ion trap reactor is estimated to be 3.0×10^{14} molecule cm^{-3}

and electrodes after the collision gas is removed (Supporting Information, Figure S3).

$$V_2O_6^- + CO \rightarrow V_2O_5^- + CO_2 \quad (5)$$

The k_1 value for the reaction of $V_2O_6^-$ with CO determined at 298 K is only 3.5×10^{-14} cm^3 $molecule^{-1}$ s^{-1}, whereas at 667 K, the k_1 value is increased to be 3.4×10^{-13} cm^3 $molecule^{-1}$ s^{-1}. The logarithm of the reaction rate constant and the reciprocal temperature have an excellent linear relationship, as shown in Figure 3. The linear equation was fitted to be $\ln k_1 = -27.0052 - 1194.88/T$ with the coefficient of determination (R^2) of 0.981126. According to the Arrhenius equation $\ln(k) = \ln(A) - E_a/(RT)$, the apparent activation energy (E_a) for Reaction (5) was determined to be 0.10 ± 0.02 eV.

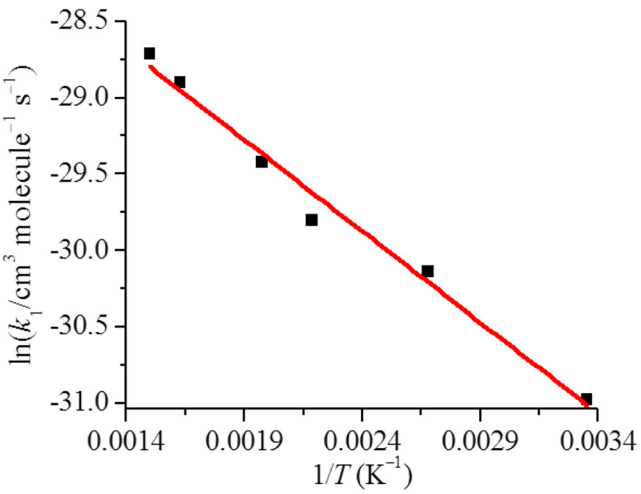

Figure 3. Arrhenius plot for the reaction of $V_2O_6^-$ with CO

DFT calculations have been performed to explore the mechanisms for the reaction of $V_2O_6^-$ with CO, and the calculated reaction pathway is presented in Figure 4. Previous studies [43] have determined that the lowest energy isomer of $V_2O_6^-$ is in the doublet state and the spin density is distributed evenly on two terminally bonded oxygen atoms, as shown in Figure 4. One of such terminal oxygen atoms can interact with CO loosely at the first step with a binding energy of only 0.03 eV (I1). Then, a positive barrier of 0.12 eV should be overcome to form the bent CO_2 unit (I1→TS1→I2). The subsequent steps are accompanied with the structure relaxation of the CO_2 unit and the final release of the gas-phase CO_2 is kinetically favorable. The rate-determining step for the reaction of $V_2O_6^-$ with CO is the formation of O–CO bond in the CO_2 unit. The calculated overall barrier of 0.12 eV is consistent with the apparent activation energy of 0.10 ± 0.02 eV determined in the experiment. This good agreement between the calculation and the experiment lends more credence to the reliability of this newly desinged high-temperature LIT reactor. In addition, the apparent activation barrier of the reaction $C_2H_5^+ + CH_4 \rightarrow C_3H_7^+ + H_2$ has been determined to be 0.14 ± 0.03 eV by our experiment, which agrees with the value of 0.11 eV reported in the literature [44] (Supporting Information, Figures S4 and S5). This agreement on the activation barrier of the $C_2H_5^+ + CH_4$ reaction further supports the reliability of our experiment.

The oxidation of CO into CO_2 is a simple but an important prototypical reaction investigaed widely in both the condensed phase [45] and the gas phase [46–49]. In the gas phase, the reactions between metal oxide clusters and CO are generally performed at room temperature [46–49]. The CO oxidation studied at higher temperatures has not been reported to the best of our knowledge. The temperature is an important factor to control the behavior of chemical reactions [8, 9], and the apparent activation energy that is closely related to the reaction rate constant can be obtained by performing the experiments at different temperatures [50]. Herein, the CO oxidation at temperatures up to 773 K was studied and the apparent activation energy of about 0.10 eV was obtained, which is consistent with theoretical calculations.

In gas-phase studies, some high-temperature experiments have been performed and very useful information has been obtained [24, 25, 51–58]. The rates of unimolecular dissociation as a function of ion temperature (about 298–500 K) have been studied by Williams et al. to obtain the apparent activation energies of large biomolecule ions [24]. Jarrold and co-workers have studied the reactions of metal clusters heated in the extension tube, such as $Al_{44}^{+/-}$ and Al_n^+ (n = 100, 114, 115, and 117), with N_2, CO_2, or C_6D_6 at different temperatures (298–1200 K), and they identify that the metal clusters in liquid phase are different in reactivity from their solid phase [51–54]. Mafuné et al. have developed a thermal desorption spectrometry that combines the mass spectrometry with a post-heating

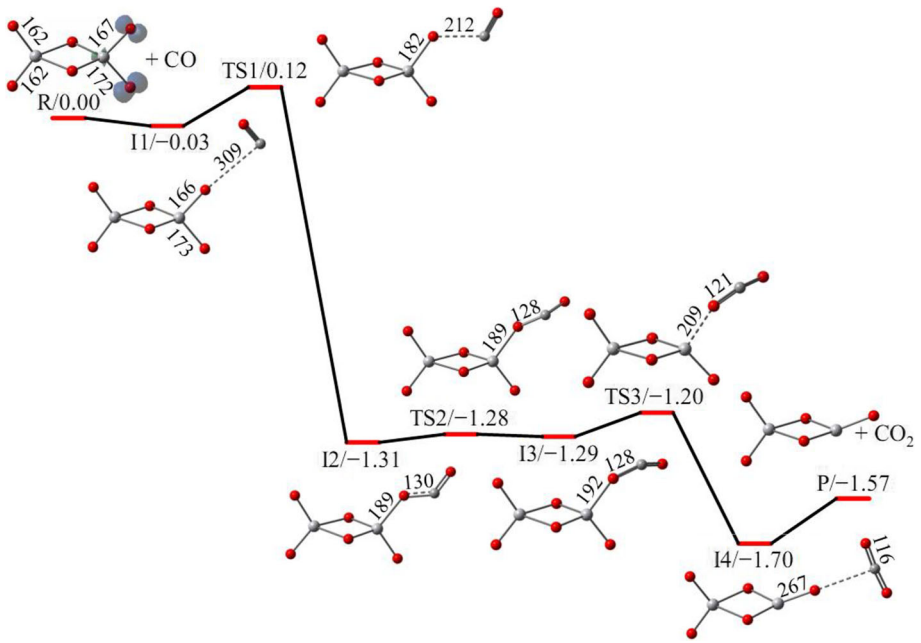

Figure 4. DFT calculated potential energy profile for the reaction of $V_2O_6^-$ with CO. The relative energies for intermediates, transition states, and products are in unit of eV. Bond lengths are given in pm

aperture. Using their experimental apparatus, they have studied the stability of various metal oxide clusters at high temperatures (300-1000 K) and the desorption of oxygen from vanadium [57], niobium [58], copper [55], rhodium [14], and palladium [56] oxide clusters have been observed. Though the high-temperature experiments have been previously performed, the chemical reactions of mass-selected and ion trap heated ions with small molecules at variable temperatures are scarcely reported. The highest temperature of such reactions reported in the literatures is about 500 K [17, 27]. Herein, the highest temperature can be up to 773 K. It is noticeable that for the reactions of ion trap heated ions, both the ions and reactant molecules are internally heated. In contrast, only the ions are internally heated in the extension tube heating experiments [51–54].

Heating the ions in the ion trap to high temperatures has to suffer from many technological difficulties and the suitable materials should be considered in the design of the ion trap. For instance, the ions in the temperature-variable quadrupole ion trap can be heated up to at most 473 K if Teflon materials are used [27]. In this study, the Al_2O_3 and SiO_2 ceramics that are stable at high temperatures were used as the electrical insulators. While the Al_2O_3 ceramic was adopted to insulate the hexapole rods and end-cap electrodes because of its good thermal conductivity, the SiO_2 ceramic was adopted to fix the ion trap assembly and decrease the thermal conduction from the ion trap assembly to vacuum chamber. This design is of great importance to guarantee the rapid thermal equilibration of the ion trap system and minimize the thermal losses. However, thermal radiation can occur through the vacuum and the power of thermal radiation is directly proportional to the fourth power of the temperature ($P = \sigma AT^4$, P is power of thermal radiation, σ is the Stefan-Boltzmann constant, A is the radiating surface area, and T is the temperature in the ion trap). As the ion trap temperature increases from 500 to 773 K, the power of thermal radiation will increase significantly (by a factor of about 6). In this design (Figure 1), the cooling water system was indispensable to protect the vacuum system of the mass spectrometer from the damage by thermal radiation. Furthermore, the inner surface of our cooling water system was plated with silver in order to improve its infrared reflectivity. With the combination of these designs, the current LIT is stable at temperatures up to 773 K. Note that higher temperatures up to 873 K have also been tested; while the system is unstable, for example, the resistive heater (Part 15, Figure 1) will be broken in a short time. In the future, new materials and designs have to be tested in order to run the LIT at higher temperatures (>773 K).

Conclusion

A high-temperature LIT has been newly designed and installed into a reflectron time-of-flight mass spectrometer coupled with a laser ablation cluster source and a quadrupole mass filter. The LIT was twined by a resistive heater and the trapped ions can be internally heated up to 773 K, which is much higher than those in similar studies. The reaction between $V_2O_6^-$ and CO has been studied at different temperatures and the apparent activation energy was determined to be 0.10 ± 0.02 eV, which is consistent with the theoretically calculated barrier of 0.12 eV. These results show that the current apparatus can be used to study the gas-phase reactions that have overall barriers.

Acknowledgments

This work was financially supported by the National Natural Science Foundation of China (Nos. 21325314 and 21303215), the Chinese Academy of Sciences (No. XDA09030101), and the Beijing Natural Science Foundation (2172059). X.-N.L. acknowledges with thanks the grant from the Youth Innovation Promotion Association, Chinese Academy of Sciences (2016030).

References

1. Koyanagi, G.K., Blagojevic, V., Bohme, D.K.: ICP-SIFT/MS study of gas-phase reactions of lanthanide cations with benzene: room-temperature kinetics and periodicities in reactivity. Int. J. Mass Spectrom. **377**, 152–158 (2015)
2. Li, Y.-K., Yuan, Z., Zhao, Y.-X., Zhao, C., Liu, Q.-Y., Chen, H., He, S.-G.: Thermal methane conversion to syngas mediated by Rh_1-doped aluminum oxide cluster cations $RhAl_3O_4^+$. J. Am. Chem. Soc. **138**, 12854–12860 (2016)
3. Yin, S., Bernstein, E.R.: Ethylene C–H bond activation by neutral mn_2o_5 clusters under visible light irradiation. J. Phys. Chem. Lett. **7**, 1709–1716 (2016)
4. O'Hair, R.A.J., Rijs, N.J.: Gas phase studies of the Pesci decarboxylation reaction: synthesis, structure, and unimolecular and bimolecular reactivity of organometallic ions. Acc. Chem. Res. **48**, 329–340 (2015)
5. Zhao, Y.-X., Liu, Q.-Y., Zhang, M.-Q., He, S.-G.: Reactions of metal cluster anions with inorganic and organic molecules in the gas phase. Dalton Trans. **45**, 11471–11495 (2016)
6. Armentrout, P.B.: Guided ion beam studies of transition metal-ligand thermochemistry. Int. J. Mass Spectrom. **227**, 289–302 (2003)
7. Armentrout, P.B., Cox, R.M.: Potential energy surface for the reaction $Sm^+ + CO_2 \rightarrow SmO^+ + CO$: guided ion beam and theoretical studies. Phys. Chem., Chem. Phys. **19**, 11075–11088 (2017)
8. Weaver, J.F., Hakanoglu, C., Antony, A., Asthagiri, A.: Alkane activation on crystalline metal oxide surfaces. Chem. Soc. Rev. **43**, 7536–7547 (2014)
9. Guo, X., Fang, G., Li, G., Ma, H., Fan, H., Yu, L., Ma, C., Wu, X., Deng, D., Wei, M., Tan, D., Si, R., Zhang, S., Li, J., Sun, L., Tang, Z., Pan, X., Bao, X.: Direct, nonoxidative conversion of methane to ethylene, aromatics, and hydrogen. Science. **344**, 616–619 (2014)
10. McLuckey, S.A., Goeringer, D.E.: Slow heating methods in tandem mass spectrometry. J. Mass Spectrom. **32**, 461–474 (1997)
11. Aguado, A., Jarrold, M.F.: Melting and freezing of metal clusters. In: Leone, S.R., Cremer, P.S., Groves, J.T., Johnson, M.A. (eds.). Annual Review of Physical Chemistry, p. 151. Annual Reviews, Palo Alto (2011)
12. Neal, C.M., Starace, A.K., Jarrold, M.F.: Ion calorimetry: using mass spectrometry to measure melting points. J. Am. Soc. Mass Spectrom. **18**, 74–81 (2007)
13. Cao, B., Starace, A.K., Judd, O.H., Bhattacharyya, I., Jarrold, M.F., Lopez, J.M., Aguado, A.: Activation of dinitrogen by solid and liquid aluminum nanoclusters: a combined experimental and theoretical study. J. Am. Chem. Soc. **132**, 12906–12918 (2010)
14. Mafune, F., Takenouchi, M., Miyajima, K., Kudoh, S.: Rhodium oxide cluster ions studied by thermal desorption spectrometry. J. Phys. Chem. A. **120**, 356–363 (2016)
15. Sakuma, K., Miyajima, K., Mafuné, F.: Oxidation of CO by nickel oxide clusters revealed by post heating. J. Phys. Chem. A. **117**, 3260–3265 (2013)
16. Viggiano, A.A., Morris, R.A., Dale, F., Paulson, J.F., Giles, K., Smith, D., Su, T.: Kinetic energy, temperature, and derived rotational temperature dependences for the reactions of $Kr^+(^2P_{3/2})$ and Ar^+ with HCl. J. Chem. Phys. **93**, 1149–1157 (1990)
17. Melko, J.J., Ard, S.G., Lê, T., Miller, G.S., Martinez, O., Shuman, N.S., Viggiano, A.A.: Determining rate constants and mechanisms for sequential reactions of Fe^+ with ozone at 500 K. J. Phys. Chem. A. **121**, 24–30 (2017)
18. Ujma, J., Giles, K., Morris, M., Barran, P.E.: New high resolution ion mobility mass spectrometer capable of measurements of collision cross-sections from 150 to 520 K. Anal. Chem. **88**, 9469–9478 (2016)
19. Kohtani, M., Jones, T.C., Schneider, J.E., Jarrold, M.F.: Extreme stability of an unsolvated α-helix. J. Am. Chem. Soc. **126**, 7420–7421 (2004)
20. Mao, Y., Woenckhaus, J., Kolafa, J., Ratner, M.A., Jarrold, M.F.: Thermal unfolding of unsolvated cytochrome *c*: experiment and molecular dynamics simulations. J. Am. Chem. Soc. **121**, 2712–2721 (1999)
21. May, J.C., Russell, D.H.: A mass-selective variable-temperature drift tube ion mobility-mass spectrometer for temperature dependent ion mobility studies. J. Am. Soc. Mass Spectrom. **22**, 1134–1145 (2011)
22. Kemper, P.R., Bowers, M.: A hybrid double-focusing mass-spectrometer-high-pressure drift reaction cell to study thermal-energy reactions of mass-selected ions. J. Am. Soc. Mass Spectrom. **1**, 197–207 (1990)
23. Servage, K.A., Silveira, J.A., Fort, K.L., Russell, D.H.: Evolution of hydrogen-bond networks in protonated water clusters $H^+(H_2O)_n$ (n = 1 to 120) studied by cryogenic ion mobility-mass spectrometry. J. Phys. Chem. Lett. **5**, 1825–1830 (2014)
24. Price, W.D., Schnier, P.D., Williams, E.R.: Tandem mass spectrometry of large biomolecule ions by blackbody infrared radiative dissociation. Anal. Chem. **68**, 859–866 (1996)
25. Asano, K.G., Goeringer, D.E., McLuckey, S.A.: Thermal dissociation in the quadrupole ion trap: ions derived from leucine enkephalin. Int. J. Mass Spectrom. **185/187**, 207–219 (1999)
26. Payne, A.H., Glish, G.L.: Thermally assisted infrared multiphoton photodissociation in a quadrupole ion trap. Anal. Chem. **73**, 3542–3548 (2001)
27. Derkits, D., Wiseman, A., Snead, R.F., Dows, M., Harge, J., Lamp, J.A., Gronert, S.: Development and evaluation of a variable-temperature quadrupole ion trap mass spectrometer. J. Am. Soc. Mass Spectrom. **27**, 339–343 (2016)
28. Bell, D.M., Howder, C.R., Johnson, R.C., Anderson, S.L.: Single CdSe/ZnS nanocrystals in an ion trap: charge and mass determination and photophysics evolution with changing mass, charge, and temperature. ACS Nano. **8**, 2387–2398 (2014)
29. Gerlich, D., Decker, S.: Trapping ions at high temperatures: thermal decay of C_{60}^+. Appl. Phys. B – Lasers Opt. **114**, 257–266 (2014)
30. Yuan, Z., Zhao, Y.-X., Li, X.-N., He, S.-G.: Reactions of $V_4O_{10}^+$ cluster ions with simple inorganic and organic molecules. Int. J. Mass Spectrom. **354/355**, 105–112 (2013)
31. Wu, X.-N., Xu, B., Meng, J.-H., He, S.-G.: C–H bond activation by nanosized scandium oxide clusters in gas phase. Int. J. Mass Spectrom. **310**, 57–64 (2012)
32. Gross, J.H.: Mass Spectrometry, 2nd edn. Springer, Berlin (2011)
33. Yuan, Z., Li, Z.-Y., Zhou, Z.-X., Liu, Q.-Y., Zhao, Y.-X., He, S.-G.: Thermal reactions of $(V_2O_5)_nO^-$ (n = 1–3) cluster anions with ethylene and propylene: oxygen atom transfer versus molecular association. J. Phys. Chem. C. **118**, 14967–14976 (2014)
34. Zhang, T., Li, Z.-Y., Liu, Q.-Y., He, S.-G.: Chemical ionization of large linear alkanes and small oxidized volatile organic compounds by the reactions with atomic gold cations. Anal. Chem. **89**, 9083-9090 (2017).
35. Frisch, M.J., Trucks, G.W., Schlegel, H.B., Scuseria, G.E., Robb, M.A., Cheeseman, J.R., Scalmani, G., Barone, V., Mennucci, B., Petersson, G.A., Nakatsuji, H., Caricato, M., Li, X., Hratchian, H.P., Izmaylov, A.F., Bloino, J., Zheng, G., Sonnenberg, J.L., Hada, M., Ehara, M., Toyota, K., Fukuda, R., Hasegawa, J., Ishida, M., Nakajima, T., Honda, Y., Kitao, O., Nakai, H., Vreven, T., Montgomery Jr., J. A., Peralta, J.E., Ogliaro, F., Bearpark, M., Heyd, J.J., Brothers, E., Kudin, K.N., Staroverov, V.N., Kobayashi, R., Normand, J., Raghavachari, K., Rendell, A., Burant, J.C., Iyengar, S.S., Tomasi, J., Cossi, M., Rega, N., Millam, J.M., Klene, M., Knox, J.E., Cross, J.B., Bakken, V., Adamo, C., Jaramillo, J., Gomperts, R., Stratmann, R.E., Yazyev, O., Austin, A.J., Cammi, R., Pomelli, C., Ochterski, J.W., Martin, R.L., Morokuma, K., Zakrzewski, V.G., Voth, G.A., Salvador, P., Dannenberg, J.J., Dapprich, S., Daniels, A.D., Farkas, O., Foresman, J.B., Ortiz, J.V., Cioslowski, J., Fox, D.J.: Gaussian 09, Revision A.1. Gaussian, Inc., Wallingford (2009)
36. Lee, C.T., Yang, W.T., Parr, R.G.: Development of the Colle-Salvetti correlation-energy formula into a functional of the electron-density. Phys. Rev. B. **37**, 785–789 (1988)
37. Becke, A.D.: Density-functional thermochemistry. 3. The role of exact exchange. J. Chem. Phys. **98**, 5648–5652 (1993)
38. Schafer, A., Huber, C., Ahlrichs, R.: Fully optimized contracted Gaussian-basis sets of triple zeta valence quality for atoms Li to Kr. J. Chem. Phys. **100**, 5829–5835 (1994)
39. Asmis, K.R., Wende, T., Brummer, M., Gause, O., Santambrogio, G., Stanca-Kaposta, E.C., Dobler, J., Niedziela, A., Sauer, J.: Structural

variability in transition metal oxide clusters: gas phase vibrational spectroscopy of $V_3O_{6-8}^+$. Phys. Chem., Chem. Phys. **14**, 9377–9388 (2012)
40. Harris, B.L., Waters, T., Khairallah, G.N., O'Hair, R.A.: Gas-phase reactions of $[VO_2(OH)_2]^-$ and $[V_2O_5(OH)]^-$ with methanol: experiment and theory. J. Phys. Chem. A. **117**, 1124–1135 (2013)
41. Berente, I., Náray-Szabó, G.: Multicoordinate driven method for approximating enzymatic reaction paths: automatic definition of the reaction coordinate using a subset of chemical coordinates. J. Phys. Chem. A. **110**, 772–778 (2006)
42. Schlegel, H.B.: Optimization of equilibrium geometries and transition structures. J. Comput. Chem. **3**, 214–218 (1982)
43. Santambrogio, G., Brümmer, M., Wöste, L., Döbler, J., Sierka, M., Sauer, J., Meijer, G., Asmis, K.R.: Gas phase vibrational spectroscopy of mass-selected vanadium oxide anions. Phys. Chem., Chem. Phys. **10**, 3992–4005 (2008)
44. Hiraoka, K., Kebarle, P.: Temperature dependence of bimolecular ion molecule reactions. The reaction $C_2H_5^+ + CH_4 = C_3H_7^+ + H_2$. J. Chem. Phys. **63**, 394–397 (1975)
45. Freund, H.-J., Meijer, G., Scheffler, M., Schlogl, R., Wolf, M.: CO oxidation as a prototypical reaction for heterogeneous processes. Angew. Chem. Int. Ed. **50**, 10064–10094 (2011)
46. Liu, Q., He, S.: Oxidation of carbon monoxide on atomic clusters. Chem. J. Chin. Univ. **35**, 665–688 (2014)
47. Li, X.-N., Yuan, Z., Meng, J.-H., Li, Z.-Y., He, S.-G.: Catalytic CO oxidation on single Pt-atom doped aluminum oxide clusters: electronegativity-ladder effect. J. Phys. Chem. C. **119**, 15414–15420 (2015)
48. Li, X.-N., Zhang, H.-M., Yuan, Z., He, S.-G.: A nine-atom rhodium-aluminum oxide cluster oxidizes five carbon monoxide molecules. Nat. Commun. **7**, 11404 (2016)
49. Wang, L.-N., Li, Z.-Y., Liu, Q.-Y., Meng, J.-H., He, S.-G., Ma, T.-M.: CO oxidation promoted by the gold dimer in $Au_2VO_3^-$ and $Au_2VO_4^-$ clusters. Angew. Chem. Int. Ed. **54**, 11720–11724 (2015)
50. Liu, Y., Su, K., Zeng, Q., Cheng, L., Zhang, L.: Decomposition reaction rate of BCl_3-CH_4-H_2 in the gas phase. Theor. Chem. Acc. **134**, 95 (2015)
51. Cao, B., Starace, A.K., Judd, O.H., Jarrold, M.F.: Melting dramatically enhances the reactivity of aluminum nanoclusters. J. Am. Chem. Soc. **131**, 2446–2447 (2009)
52. Leslie, K.L., Jarrold, M.F.: Dehydrogenation of benzene on liquid Al_{100}^+. J. Phys. Chem. A. **117**, 2075–2081 (2013)
53. Leslie, K.L., Shinholt, D., Jarrold, M.F.: Reactions of CO_2 on solid and liquid Al_{100}^+. J. Phys. Chem. A. **117**, 1053–1058 (2013)
54. Cao, B., Starace, A.K., Judd, O.H., Bhattacharyya, I., Jarrold, M.F.: Reactions of liquid and solid aluminum clusters with N_2: the role of structure and phase in Al_{114}^+, Al_{115}^+, and Al_{117}^+. J. Chem. Phys. **141**, 204304 (2014)
55. Mafuné, F., Miyajima, K., Morita, K.: Release of oxygen from copper oxide cluster ions by heat and by reaction with NO. J. Phys. Chem. C. **119**, 11106–11113 (2015)
56. Miyajima, K., Mafuné, F.: Release of oxygen from palladium oxide cluster ions by heat. J. Phys. Chem. A. **119**, 8055–8061 (2015)
57. Kurokawa, H., Mafuné, F.: Thermal desorption of oxygen from near-stoichiometric cationic vanadium oxide clusters. Chem. Phys. Lett. **651**, 24–27 (2016)
58. Masuzaki, D., Nagata, T., Mafuné, F.: Desorption of oxygen from cationic niobium oxide clusters revealed by gas phase thermal desorption spectrometry and density functional theory calculations. J. Phys. Chem. A. **121**, 2079–2085 (2017)